IEEE Access
Multidisciplinary ⋮ Rapid Review ⋮ Open Access Journal

Received April 9, 2018, accepted May 17, 2018, date of publication May 25, 2018, date of current version June 20, 2018.

Digital Object Identifier 10.1109/ACCESS.2018.2840535

Maximizing Throughput of Hybrid FSO-RF Communication System: An Algorithm

MUHAMMAD NASIR KHAN[1,2], SYED OMER GILANI[1], MOHSIN JAMIL[1,3], ABDUL RAFAY[1], QASIM AWAIS[4], BILAL A. KHAWAJA[3,5], MUHAMMAD UZAIR[3], AND ABDUL WAHEED MALIK[6]

[1]Department of Robotics and AI, National University of Sciences and Technology, Islamabad 44000, Pakistan
[2]Department of Electrical Engineering, The University of Lahore, Lahore 54000, Pakistan
[3]Department of Electrical Engineering, Faculty of Engineering, Islamic University of Madinah, Medina 41411, Saudi Arabia
[4]Department of Optoelectronic Engineering, Chongqing University, Chongqing 400044, China
[5]Department of Electronic and Power Engineering, PN-Engineering College, National University of Sciences and Technology, Karachi 74200, Pakistan
[6]Department of Electrical Engineering, COMSATS University Islamabad, Abbottabad 44000, Pakistan

Corresponding author: Muhammad Nasir Khan (muhammad.nasir@ee.uol.edu.pk)

ABSTRACT Electromagnetic spectrum is too cluttered to add additional broadband channels of high data rate and bandwidth. Free space optical (FSO) communication is one of the most dominant optical wireless communication systems, which provides huge and licensed free spectrum, non-interfering link, and high data rate. Despite of having above-mentioned advantages, the FSO links are very sensitive to bad weather conditions (i.e., fog, snow, dust, and their combination). Therefore, there is a dire requirement to develop a system that can overcome issues of individual communication system and adjust the current demand of new broadband channels. Adaptive FSO-radio frequency (RF) communication system is proposed to tackle the individual channel issues. A novel throughput maximization algorithm (TMA) is developed for the adaptive hybrid FSO-RF channel. Performance of the proposed algorithm for adaptive hybrid communication system is analyzed considering the regular and right-regular low density parity check (LDPC) code under various weather conditions. Simulation results show that the TMA performs well under all weather conditions and gives a performance gain of up to 2.25 dB considering the right-regular LDPC code. From the presented results, it is also seen that the suggested communication system optimizes mapping schemes, bit proportions for each channel, and puncturing ratios adaptively for different degree variable nodes in worst weather conditions.

INDEX TERMS Throughput maximization algorithm (TMA), low density parity check code (LDPC), extrinsic mutual information transfer (EXIT).

I. INTRODUCTION

From the last few decades, the radio frequency (RF) communications have gained market interest because of its enormous benefits [1]. However, there are many limitations (e.g.,spectrum in-efficiency and licensing cost), which impose challenges for deployment of additional broadband channels in the existing electromagnetic spectrum [2]. Bandwidth hungry applications and high data rate is the current market demand. Therefore, there is a dire need to have an alternative band, which supports channels requiring high bandwidth. Free space optical (FSO) communication is a promising technology, which offers huge and unregulated spectrum with many inherited benefits [1], [3]–[6]. These benefits are high data rate, non-interfering nature, highly secured links and easy to install. However, despite having such great benefits, FSO also suffers from many drawbacks [7]. These drawbacks are line-of-sight (LOS) requirement, limited distance and severely affected by worse weather conditions (i.e.,fog and snow).

The reliability and connectivity of FSO link is highly weather dependent, which greatly degrades the system performance. The reliability or robustness of a communication system can be defined as the ability to maintain certain system performances under worse channel conditions [8]. Recently many ideas have been put forward by research community to overcome issues of both technologies (i.e., RF and FSO) [9]–[16]. These ideas are in the form of hybrid communication system, which work differently for different systems. It was suggested to have independent links and also dependent links with different scenarios of deployment. Each system has its own merits and demerits. The major contributions are as under;

- Hybrid free space optical (FSO)/radio frequency (RF) communication system is proposed to meet the current demands of high data rate and link availability. We have previously mentioned the hybrid FSO/RF communication system in [17] and [18]. In the previous work [18], adaptive systems considering power optimization rules were discussed. The focus was to transmit maximum power through good channel (e.g., good weather) and minimum power through bad channel (e.g., bad weather). Khan and Jamil [18] evaluate the proposed communication system over simple channel for a given fixed code rate. A single pair of encoder and decoder is considered and extrinsic information transfer (EXIT) chart [19] is used to evaluate the performance of coded system. Having a single encoder and decoder pair is the main advantage (i.e., no synchronization issue and cost effective) of the proposed communication system and variations in channel conditions on both links are adapted by introducing puncturing technique. In the present work, we suggest low density parity check (LDPC) code and are optimizing rate parameter by introducing the puncturing technique. A puncturing optimization algorithm (POA) [17] is employed for the optimization purpose and optimization is performed such as to maximize the throughput (i.e., information bits). According to the best of our knowledge no such analysis is done in the literature. In literature [12], [20], and [21], they consider hybrid system and have suggested some combining techniques for the hybrid FSO/RF communication system with different aspect.
- Secondly, a throughput maximization algorithm (TMA) is developed for the hybrid FSO/RF communication system considering the regular as well as irregular structure of LDPC code. The idea is to optimize the bit fraction and try to exploit that channel, which have clear sky conditions. While doing the optimization, the proposed algorithm considers two cases:-partially optimized and fully optimized. In partially optimized case, only puncturing fractions are optimized while for the fully optimized case both puncturing fractions and modulation sizes are optimized for each degree of variable node (VN). Most recent work about the performance of hybrid FSO/RF communication system is found in [20] and [21]. The work in [20] is particularly proposed for the situation where direct link between user and base station in not possible. In [21], they are suggesting the hybrid FSO/RF communication system model with receive diversity. But we are focusing the development of novel algorithm which maximizes the proportion of bits transmitted through each channel depending on different weather conditions.
- For the validation of the proposed system, we provide numerical and theoretical analysis. It is seen that the proposed system well optimizes the varying channel conditions and provides transmission reliability over wide range of rates. Analysis and simulation results are provided to support the proposed system. We then extend the algorithm for the quaternary modulations scheme for the hybrid FSO/RF channel. For this we analyze the demapper EXIT curves for different mapping schemes (gray and anti-gray). We provide investigations for 4-PAM and QPSK EXIT over varying channel conditions. Then we simulate the overall EXIT chart curve for the hybrid FSO/RF channel. Since we consider the parallel channel, we also measure the best possible fraction of bits to be transmitted to the respective channel.

II. PROPOSED COMMUNICATION SYSTEM MODEL

Hybrid FSO-RF communication system model, which consists of a parallel RF and optical link, is shown in Fig. 1. At the transmitter side, k information bits are encoded into n bits codeword with a certain code rate. The coded bits are divided into two streams (i.e., $n_o = nf$ bits are sent through the optical channel and $n_r = n(1-f)$ bits are sent through RF channel), where f is bit division factor, which is dependent on channel conditions and transmission schemes on each link. The respective channel bits are further multiplexed into I streams (i.e., for different degrees in case of irregular LDPC code) depending on the VN degree. Channel bits are then mapped accordingly using either of the mapping scheme (i.e., from M-level amplitude modulation (M-PAM) for optical channel and M-level phase shift keying (M-PSK) for RF channel). The mapped symbols of the respective channel stream are punctured in a random fashion and transmit unpunctured symbols $\left(\frac{n_o}{\log_2|\mathcal{X}|}(1-p), \frac{n_r}{\log_2|\widehat{\mathcal{X}}|}(1-\widehat{p})\right)$ over the respective link, where $p(\widehat{p})$ denote optical(RF) channel puncturing fraction. It is assumed that optical and RF symbols are drawn uniformly with unit energy from given constellations. On each channel zero mean with unit variance noise (i.e., additive white Gaussain noise (AWGN) $\sim \mathcal{N}(0, 1)$) is added.

An AWGN RF channel and a log-normally (LN) faded optical channel is considered. The LN fading distribution is given by [22], whose strength is characterized by an entity known as scintillation index (SI). At the receiver side, received optical and RF signals from different degree VNs corresponding to optical and RF channels are de-multiplexed, de-punctured, de-mapped and decoded to extract the original message with certain error probability. The code rate for different channel conditions is determined by channel state information (CSI), which is known at the transmitter.

A. OPTICAL CHANNEL MODEL

The optical channel exploits intensity modulation with direct detection (IM/DD) using the available transmission schemes

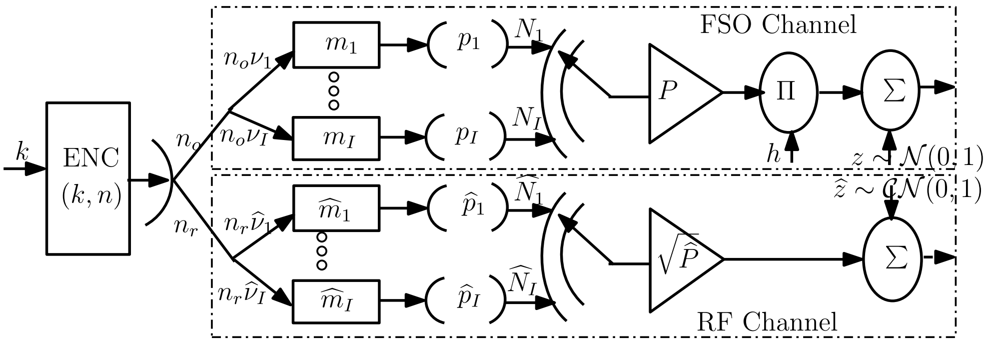

FIGURE 1. Rate Adaptive Hybrid FSO-RF Communication System.

(i.e., in our case either of the 2-PAM or 4-PAM). The collected noisy signal after the optical to electrical conversion is given by,[1]

$$y = Phx + z, \tag{1}$$

where $x \in \mathcal{X}$ denotes transmitted optical symbols, h denotes optical channel fading given in [22] and [23, eq. (5)], P represents average received optical signal power and z is the channel noise. Due to the uni-polar nature of optical signals and PAM mapping schemes, the DC component of noisy electrical signal can be neglected, which is equivalent ±1 for 2-PAM and $\{-1, -1/3, +1/3, +1\}$ for 4-PAM for the same optical power P. Signal to noise ratio (SNR) for 2-PAM is calculated as $\gamma = P^2$ (after AC coupling) and is $\gamma = \frac{5}{9}P^2$ for 4-PAM.

B. RF CHANNEL MODEL

The transmission of RF symbols is done by considering the given transmission schemes (i.e., in our case either of BPSK or QPSK), assuming a fading free AWGN channel with RF signal power $\widehat{P}$ and the received RF noisy signal is,

$$\widehat{y} = \sqrt{\widehat{P}}\widehat{x} + \widehat{z}, \tag{2}$$

where $\widehat{x} \in \widehat{\mathcal{X}}$ denotes transmitted RF symbols, $\widehat{z}$ represents a zero mean and unit variance AWGN. SNR in this case is $\widehat{\gamma} = \widehat{P}$.

III. THROUGHPUT MAXIMIZATION ALGORITHM (TMA)

The research objective is to maximize the throughput (k bits per hybrid symbol) of hybrid FSO-RF communication system over varying channel conditions. In TMA, puncturing fractions and mapping schemes[2] are optimized according to varying channel scenarios. The proposed TMA is flexible in terms of its implementation for a regular as well as for irregular LDPC code.

In optimization problem, two EXIT curves are generated, one curve corresponds to variable node decoder (VND) and second corresponds to check node decoder (CND). In the objective function, minimum positive difference (MPD) rule given by [17, eq. (11)] is followed for the evaluation of VND and CND EXIT curves. The MPD rule is used to find the best throughput and corresponding optimum puncturing fractions. The VND EXIT curve depends on the degree of VN, channel SNR and characteristics of mapping schemes. The CND EXIT curve depends only on the degree of check node (CN). We consider $d_{v,i}$ different degree VN, where $i = 1, \cdots, d_{v,max}$. The fraction of VN having degree $d_{v,i}$ is denoted by ν_i, while the fraction of edges incident on VN of degree $d_{v,i}$ is represented by ϑ_i.

A. REGULAR LDPC CODE

In a regular structure LDPC code, only two channels (i.e., optical and RF) are considered with varying mapping scheme and puncturing fractions of same degree VN. For regular LDPC code, a single stream of FSO and RF channel representing a fixed VN degree is considered. In such case, codeword of n bits is divided into two streams (i.e., one for optical and other for RF link) is,

$$n \triangleq n_o + n_r, \tag{3}$$

where $n_o = nf$, $n_r = n\widehat{f}$, $\widehat{f} = (1-f)$ and $f(\widehat{f})$ is the bit division factor depending on the optical(RF) channel condition. A more generic system is considered and it would be independent on actual block length (e.g., n) of encoded bit for the sake of simplicity in simulating the system. But the practical meaning of $f(\widehat{f})$ are same as are mentioned earlier. After implementing mapping and puncturing, optical channel bits are given by,

$$n_o = nf = \frac{Nm}{(1-p)}, \tag{4}$$

where N (i.e., number of symbols being transmitted on optical channel), p is the fraction of optical channel symbols being punctured and $m = \log_2(\mathcal{M})$ optical bits per symbol. Similarly RF channel bits are given by,

$$n_r = n\widehat{f} = \frac{\widehat{N}\widehat{m}}{(1-\widehat{p})}, \tag{5}$$

[1] For the sake of simplicity, photo-detector's efficiency constant scaling coefficient has been ignored from (1).

[2] To avoid later confusion of mapping with bit labelling, here, mapping means modulations sizes either binary or quaternary.

where $\widehat{N}$ (i.e., number of symbols being transmitted on RF channel), $\widehat{p}$ is fraction of RF channel symbols being punctured and $\widehat{m} = \log_2(\widehat{\mathcal{M}})$ RF bits per symbol. By adding (4) and (5),

$$n = \left(\frac{Nm}{(1-p)} + \frac{\widehat{N}\widehat{m}}{(1-\widehat{p})}\right). \tag{6}$$

Over a defined constraint of same symbol rate for the optimization problem, i.e., $N = \widehat{N} = N_H$, (6) is further simplified to,

$$n = N_H\left(\frac{m}{1-p} + \frac{\widehat{m}}{1-\widehat{p}}\right), \tag{7}$$

where N_H is the total number of hybrid symbols. Since $k = nR_m$ (R_m is the mother code rate), then throughput for regular LDPC code is,

$$k = R_m N_H\left(\frac{m}{1-p} + \frac{\widehat{m}}{1-\widehat{p}}\right). \tag{8}$$

The optical channel bit fraction f for regular LDPC code depends on the mapping scheme as well as on puncturing fractions of both channels and is derived as follows:

From (4) and (5), it is easy to find the number of symbols transmitted through optical and RF channel as,

$$N = \frac{nf(1-p)}{m}. \tag{9}$$

$$\widehat{N} = \frac{n(1-f)(1-\widehat{p})}{\widehat{m}}. \tag{10}$$

Given the constraint of same symbol rate, (9) and (10) can be compared to give,

$$\frac{f}{1-f} = \frac{m(1-\widehat{p})}{\widehat{m}(1-p)}. \tag{11}$$

Substituting $\mathcal{S} = \frac{m(1-\widehat{p})}{\widehat{m}(1-p)}$ in (11), optical channel bit fraction is calculated as,

$$f = \frac{\mathcal{S}}{1+\mathcal{S}}. \tag{12}$$

The *TMA* objective function in case of regular LDPC code is,

$$\begin{cases} \textit{Maximize}: & k = R_m N_H\left(\frac{m}{1-p} + \frac{\widehat{m}}{1-\widehat{p}}\right), \\ \textit{Constraints}: & 1: \ 0 \le \vec{p} \triangleq [p, \widehat{p}] \le 1, \\ & 2: f + \widehat{f} = 1, \qquad f \ge 0, \widehat{f} \ge 0, \\ & 3: f\left(\frac{1-p}{m}\right) = \widehat{f}\left(\frac{1-\widehat{p}}{\widehat{m}}\right), \\ & 4: \mathcal{I}_{EV,H}(\widehat{\mathcal{I}}_{dm,e}, \mathcal{I}_{dm,e}, d_v, \vec{p}, \mathcal{I}_{AV}) > \\ & \qquad \mathcal{I}_{AC}(d_c, \mathcal{I}_{EC} = \mathcal{I}_{AV}), \end{cases} \tag{13}$$

where $\mathcal{I}_{dm,e}$ and $\widehat{\mathcal{I}}_{dm,e}$ denote de-mapper characteristics of optical and RF channels respectively, $\vec{p} \triangleq [p, \widehat{p}]$ is the puncturing fraction pair on optical(RF) channel, $\mathcal{I}_{EV,H}$ is the overl VND extrinsic MI, d_v represent VN degree, $\mathcal{I}_{AV}(\mathcal{I}_{AC})$ denote the a-priori VN(CN) MIs, $\mathcal{I}_{EC}$ is the CND extrinsic MI and d_c denotes the CN degree. The de-mapper characteristics curve is evaluated following the same method given in [17].

In (13),

1) ensures positive puncturing fractions on both channel;
2) ensures an appropriate division of coded bits on each channel, which is a function of puncturing fractions and mapping;
3) defines same symbol rate constraint for hybrid channel; and
4) permits the opening of tunnel between two EXIT curves (i.e., VND and CND) for successful decoding.

The overall VND curve $\mathcal{I}_{EV,H}$ depends on mapping scheme, degree of VNs and respective channel SNR. The overall extrinsic mutual information (MI) for regular LDPC code is given by,

$$\begin{aligned} \mathcal{I}_{EV,H}(\widehat{\mathcal{I}}_{dm,e}, \mathcal{I}_{dm,e}, d_v, \vec{p}, \mathcal{I}_{AV}) &= f\mathcal{I}_{EV}\left(\mathcal{I}_{AV}, \mathcal{I}_{dm,e}, d_v\right) \\ &\quad + \widehat{f}\widehat{\mathcal{I}}_{EV}\left(\mathcal{I}_{AV}, \widehat{\mathcal{I}}_{dm,e}, d_v\right), \end{aligned} \tag{14}$$

where $\mathcal{I}_{EV}$ and $\widehat{\mathcal{I}}_{EV}$ are VND extrinsic MIs corresponding to optical and RF channel respectively. The VND extrinsic MI is evaluated using [17, eq. (12)] in which ξ is,

$$\xi = \mathcal{J}\left(\sqrt{\psi + [\mathcal{J}^{-1}(\mathcal{I}_{dm,e})]^2}\right), \tag{15}$$

where in (15), $\psi = (i-1)[\mathcal{J}^{-1}(\mathcal{I}_{AV})]^2$ and $\mathcal{I}_{dm,e}(P, \mathcal{I}_{dm,a})$ depends on optical power and *a-priori* MI from VN corresponding to optical channel. Similarly $\widehat{\mathcal{I}}_{dm,e}(\widehat{P}, \widehat{\mathcal{I}}_{dm,a})$ depends on RF power and *a-priori* MI from VN corresponding to RF channel. The de-mapper extrinsic MI is calculated using the same procedure given in [17].

B. RIGHT-REGULAR LDPC CODE

In right-regular LDPC code, multiple channel streams on both links are considered. Throughput optimization function and bit fraction for both links is analyzed assuming right-regular LDPC code. A special case with degree 2 and 4 VN for right-regular LDPC code is considered as shown in Fig. 2.

Following the same procedure as is done in subsection III-A, (7) can be derived for right-regular LDPC code as,

$$n = \left[\frac{N_2 m_2}{(1-p_2)} + \frac{N_4 m_4}{(1-p_4)}\right] + \left[\frac{\widehat{N}_2\widehat{m}_2}{(1-\widehat{p}_2)} + \frac{\widehat{N}_4\widehat{m}_4}{(1-\widehat{p}_4)}\right], \tag{16}$$

where $\nu_2(\widehat{\nu}_2)$ and $\nu_4(\widehat{\nu}_4)$ are fractions of optical(RF) coded bits corresponding to degree 2 and 4 VNs respectively, $N_2(\widehat{N}_2)$ and $N_4(\widehat{N}_4)$ denote the number of symbols corresponding to degree 2 and 4 VNs, being transmitted on the optical(RF) channel, $p_2(\widehat{p}_2)$ and $p_4(\widehat{p}_4)$ are the puncturing fractions of degree 2 and 4 variable nodes corresponding to optical(RF) link. Having an assumption of same symbol rate constraints, i.e., $N = N_2 + N_4$ and $\widehat{N} = \widehat{N}_2 + \widehat{N}_4$, (8) for right regular LDPC code structure is,

$$\begin{aligned} k = R_m\Bigg[&\left(\frac{N_2 m_2}{(1-p_2)} + \frac{(N-N_2)m_4}{(1-p_4)}\right) \\ &+ \left(\frac{\widehat{N}_2\widehat{m}_2}{(1-\widehat{p}_2)} + \frac{(\widehat{N}-\widehat{N}_2)\widehat{m}_4}{(1-\widehat{p}_4)}\right)\Bigg]. \end{aligned} \tag{17}$$

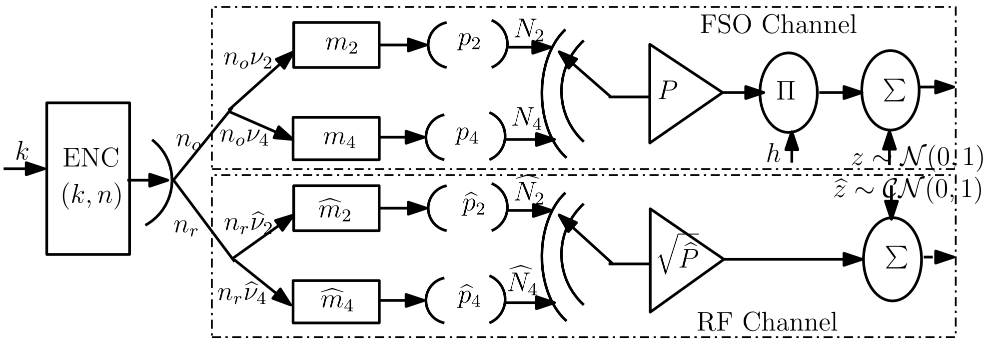

FIGURE 2. Extension of Fig. 1, Right-regular LDPC code structure with degree 2 and 4 VN.

The objective function can directly be evaluated using EXIT chart with greater speed and less computational complexity. Optimization problem, which is based on EXIT chart analysis is often independent on codeword block length. However, throughput given by (17) is dependent on the codeword block length, which is not directly analyzed using EXIT chart. To evaluate (17), optimization problem needs to run a large number of Monte Carlo (MC) simulations, which is not feasible. Therefore, (17) should be derived such that it must be independent of block length.

The number of channel symbols transmitted through degree 2 and 4 VNs are given by,

$$N_2 = \frac{n_o(1-p_2)}{m_2}. \quad (18)$$

$$N_4 = \frac{n_o(1-p_4)}{m_4}. \quad (19)$$

Considering the same symbol rate constraint, i.e., $N = N_2 + N_4$ and by re-arranging (18) and (19),

$$N = n_o\left[\frac{(1-p_2)}{m_2} + \frac{(1-p_4)}{m_4}\right]. \quad (20)$$

Similarly for RF channel,

$$\widehat{N} = n_r\left[\frac{(1-\widehat{p}_2)}{\widehat{m}_2} + \frac{(1-\widehat{p}_4)}{\widehat{m}_4}\right]. \quad (21)$$

From (20) and (21),

$$n_o = N\left[\frac{m_2 m_4}{[m_4(1-p_2)+m_2(1-p_4)]}\right]. \quad (22)$$

$$n_r = \widehat{N}\left[\frac{\widehat{m}_2\widehat{m}_4}{[\widehat{m}_4(1-\widehat{p}_2)+\widehat{m}_2(1-\widehat{p}_4)]}\right]. \quad (23)$$

Using (22), (23), (3) in $k = nR_m$ and considering $N = \widehat{N} = N_H$,

$$k = R_m N_H\left[\left(\frac{m_2 m_4}{[m_4(1-p_2)+m_2(1-p_4)]}\right) + \left(\frac{\widehat{m}_2\widehat{m}_4}{[\widehat{m}_4(1-\widehat{p}_2)+\widehat{m}_2(1-\widehat{p}_4)]}\right)\right]. \quad (24)$$

The bit fraction f for right-regular LDPC code depends on mapping schemes corresponding to different degree VNs and puncturing ratios. Using $N = N_2+N_4$, (9) is derived in terms of a right-regular LDPC code as,

$$N = nf\left(\frac{(1-p_2)}{m_2} + \frac{(1-p_4)}{m_4}\right). \quad (25)$$

Similarly using $\widehat{N} = \widehat{N}_2 + \widehat{N}_4$, (10) is derived in terms of right-regular LDPC code as,

$$N_r = n(1-f)\left(\frac{(1-\widehat{p}_2)}{\widehat{m}_2} + \frac{(1-\widehat{p}_4)}{\widehat{m}_4}\right). \quad (26)$$

Substituting

$$\mathcal{U} = \left(\frac{(1-p_2)}{m_2} + \frac{(1-p_4)}{m_4}\right) \quad \text{and}$$
$$\widehat{\mathcal{U}} = \left(\frac{(1-\widehat{p}_2)}{\widehat{m}_2} + \frac{(1-\widehat{p}_4)}{\widehat{m}_4}\right)$$

in (25) and (26) respectively,

$$f = \frac{\widehat{\mathcal{U}}}{\widehat{\mathcal{U}}+\mathcal{U}}. \quad (27)$$

The objective function of *TMA* in case of right-regular LDPC code is,

$$\begin{cases} \textit{Maximize}: & \max (24), \\ \textit{Constraints}: & 1: 0 \le \vec{p} \triangleq [p_2, p_4, \widehat{p}_2, \widehat{p}_4] \le 1, \\ & 2: f+\widehat{f} = 1, \qquad f \ge 0, \widehat{f} \ge 0, \\ & 3: f\left(\frac{(1-p_2)}{m_2} + \frac{(1-p_4)}{m_4}\right) \\ & \quad = \widehat{f}\left(\frac{(1-\widehat{p}_2)}{\widehat{m}_2} + \frac{(1-\widehat{p}_4)}{\widehat{m}_4}\right), \\ & 4: \mathcal{I}_{EV,H}(\mathcal{I}_{dm,e}, \mathcal{I}_{dm,e}, d_{v,i}, \vec{p}, \mathcal{I}_{AV}) \\ & \qquad > \mathcal{I}_{AC}(d_c, \mathcal{I}_{EC} = \mathcal{I}_{AV}). \end{cases} \quad (28)$$

The overall VND curve $\mathcal{I}_{EV,H}$ depends on mapping scheme, degree of VNs and respective channel SNR. The overall extrinsic MI for right-regular LDPC code is given by (29), as shown at the top of the next page, where $d_{v,i}$ denotes i-th VN degree and ϑ_i denotes the edge fraction incident on i-th degree VN corresponding to optical and RF link.

$$\mathcal{I}_{EV,H}(\widehat{\mathcal{I}}_{dm,e}, \mathcal{I}_{dm,e}, d_{v,i}, \vec{p}, \mathcal{I}_{AV}) = f\sum_{i_{FSO}} \vartheta_i \mathcal{I}_{EV}\left(\mathcal{I}_{AV}, \mathcal{I}_{dm,e}, d_{v,i}\right) + \widehat{f}\sum_{i_{RF}} \vartheta_i \widehat{\mathcal{I}}_{EV}\left(\mathcal{I}_{AV}, \widehat{\mathcal{I}}_{dm,e}, d_{v,i}\right), \tag{29}$$

IV. DE-MAPPER EXIT CHART ANALYSIS TECHNIQUES

As is mentioned in Section II, at the transmitter side, information bits are encoded with a certain code rate and generates a codeword for transmission. The codeword is then fed to mapper[3] which then converts coded bits into symbols and each symbol is either real or complex depending on the type of mapper (optical and/or RF).

At the receiver side, noisy received signal is detected at the input of de-mapper. Main components of receiver are de-mapper and decoder, each of which is implemented using soft values (i.e., log-likelihood ratios (LLRs)). Conventionally, they are connected with interleavers and de-interleavers. In simulations, we do not implement interleavers and de-interleavers because of the randomness created by the parity-check matrix itself. The received symbols are then passed through the de-mapper. The de-mapper performs de-mapping and produces soft values ($\Lambda_{dm,e}$), which are known as *extrinsic* LLRs of de-mapper. Soft values are then fed in to decoder and are known as the decoder's *a-priori* LLR. The decoder works on the standard sum-product algorithm (SPA) [25]. The output of decoder ($\Lambda_{d,e}$) is used as de-mapper's *a-priori* LLR. This whole process of backward and forward is known as iterative process between de-mapper and decoder. The corresponding closed form expressions of LLR for AGM is challenging. Therefore, in order to solve de-mapper extrinsic MI considering AGM for the above defined optimization problem, we exploit two approaches: *Curve Fitting* and *Lookup Table*.

A. CURVE FITTING TECHNIQUE

Curve fitting (CF) technique is a well-known technique adopted by many researchers [26], [27] for fast approximation of a problem with unknown closed form solution. To calculate extrinsic MI of de-mapper assuming AGM scheme is very challenging and the best way is to use CF technique to speed up calculations. EXIT chart of de-mapper without known closed form expressions is calculated using CF technique. In this technique, we evaluate EXIT chart of de-mapper using [17, eq. (16)] and store evaluated results in the form of polynomials and are used in optimization problem.

MC simulations are performed using [17, eq. (16)] to calculate de-mapper extrinsic MI over a large range of respective channel powers $P^\star$.[4] The generalized form of polynomial function stored using CF technique is,

$$\mathcal{I}^\star_{dm,e}\left(P^\star, d_v, \mathcal{I}_{AV}\right) = \sum_i \mathcal{T}_i \mathcal{I}^i_{AV}, \tag{30}$$

where $\mathcal{T}_i$ denotes coefficients of i-th order polynomial and it depends on powers of corresponding channel (i.e., optical(RF)) and degree of VNs. The advantage of using this technique is to expedite algorithm speed and minimize computational complexity. On the other hands, this technique has disadvantage as well, i.e., *firstly*, it is not capable of doing any extrapolation and *secondly*, it is not a memory flexible.

B. LOOKUP TABLE

Lookup Table (LT) technique is also known as interpolation and is adopted by many researchers [28, and reference therein]. The LT technique requires only a small amount of off-line computation and storage of necessary data. The difference in LT technique is that interpolation points are used rather than coefficients of polynomials. The generalized form of results stored using LT technique is given by (31), as shown at the bottom of the next page.

The process of LT involves semi-analytic design procedure and it avoids time consuming MC simulations over a large range of puncturing ratios. Using LT technique, computational complexity is minimized and speed of proposed algorithm is maximized. The LT technique is capable of doing extrapolations as well. Therefore, with extrapolation capability of LT, we can get results over larger step size without increasing memory size and re-computing MC simulations.

C. NUMERICAL RESULTS

Numerical example is presented using half rate regular $\langle 3, 6\rangle$-LDPC code assuming a single RF channel. In this example, quaternary modulation assuming GM/AGM schemes is considered. MC simulations are performed and store parameters both for CF and LT technique over a large range of powers on respective channels. The comparison of CF, LT and MC simulation is presented in Fig. 3. Figure 3 shows that results obtained using MC simulations, CF and LT technique agree well for a given SNR.

V. TMA PERFORMANCE COMPARISON

The performance of proposed algorithm considering regular and right-regular LDPC code is measured over the adaptive hybrid FSO(RF) communication system. Note that for regular LDPC code, adaptive hybrid system optimizes puncturing ratios and mapping scheme on both channels using objective

[3]The mapper, $\mathcal{M}(\widehat{\mathcal{M}})$, inputs a block of $m(\widehat{m})$-bits and maps them into symbols either for optical or RF channel depending on the constellation sizes on each channel. Specifically, gray/anti-gray mapping (GM/AGM) is considered in which the bit labelling for quaternary modulation is [00, 01, 11, 10] assuming GM and [00, 01, 10, 11] assuming AGM. Simply, GM means that two symbols at minimum Euclidean distance only differ by one bit, while AGM means that symbols are numbered from 0 to $\mathcal{M}$-1 [24].

[4]Power and MI notations with $\star$ mark are used to show correspondence of both parameters, i.e., Optical(RF) powers and de-mapper extrinsic MI in a similar fashion and define $P^\star$ as $P^\star \triangleq (P, \widehat{P})$ and $\mathcal{I}^\star_{dm,e}$ as $\mathcal{I}^\star_{dm,e} \triangleq (\mathcal{I}_{dm,e}, \widehat{\mathcal{I}}_{dm,e})$.

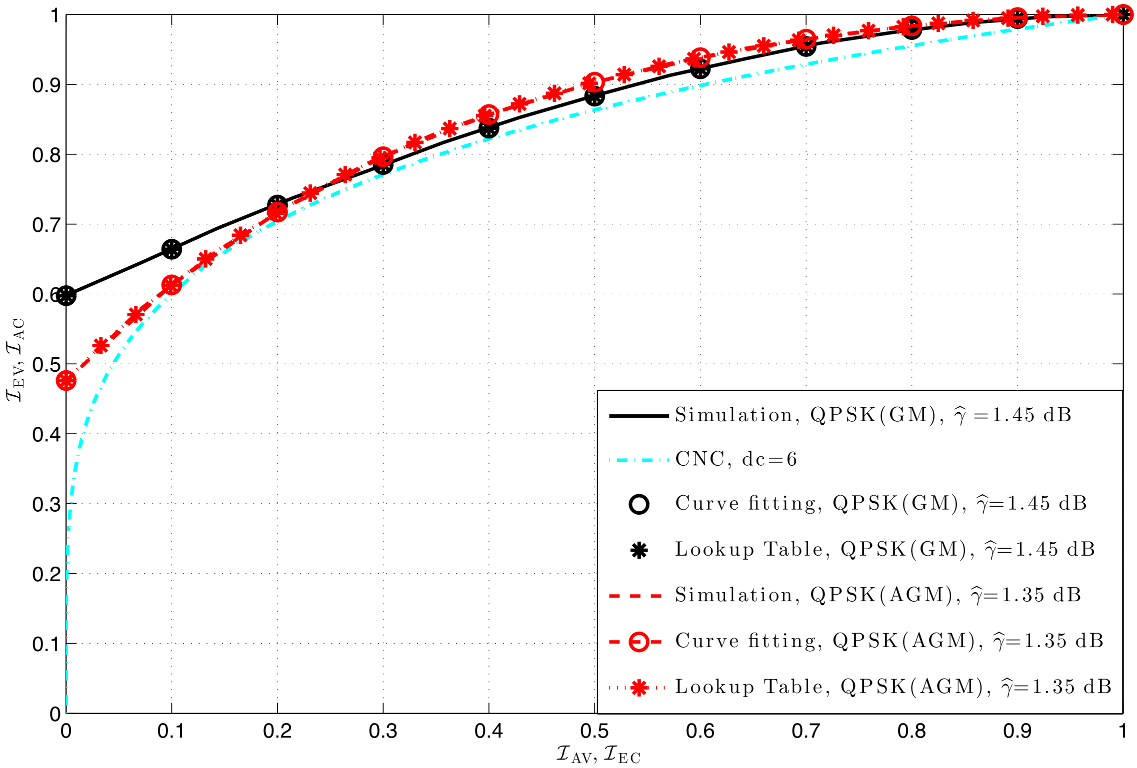

FIGURE 3. EXIT chart for single AWGN RF channel using QPSK transmission scheme and half rate regular (3, 6)-LDPC code, where $\hat{\gamma} = \hat{P}$.

function given by (13). The objective function gives maximum throughput and the corresponding optimized puncturing ratios under varying channel conditions. For right-regular LDPC code, two different cases are considered for optimization:

1) **Partially optimized**: In this case of right-regular structure with *partial* optimization, adaptive hybrid system optimizes puncturing ratios for different degrees VN while keeping optimized mapping identical for each degree (e.g., if optimization function given by (28) selects binary modulation for optical channel, then according to *partial* optimization, assign binary modulation to both degrees 2 and 4. Similarly if optimization function selects quaternary modulation for optical channel, then assign quaternary modulation to both degrees 2 and 4. Same procedure is true for the radio channel).
2) **Fully optimized**: In this case, adaptive hybrid system optimizes puncturing ratio and modulation sizes for each degree VN of the respective channel. The objective function selects optimized modulation sizes as well as corresponding puncturing ratios for degree 2 and 4 VNs on each channel (i.e., optical(RF)), which give the best throughput.

Simulation results are presented in Fig. 4 assuming regular and right-regular structure, whose objective functions are given by (13) and (28) respectively. AGM bit labelling is considered for QPSK and 4-PAM. The performance gain is observed, when system moves from regular to right-regular structure and also from binary to non-binary modulation schemes. It is seen from optimization results in Fig. 4 that the proposed algorithm flexibly adopts varying channel conditions (i.e., it flexibly distributes proportion of bits on each link (optical(RF)) under varying channel conditions).

It is seen that using right-regular structure with partial optimization, 1.25 dB optical power gain is achieved as compared to regular structure at $k = 1$ bits per hybrid symbol (i.e., when adaptive system selects binary modulation for both channels). The performance gain improves further on selecting non binary modulation scheme. It is also observed from Fig. 4 that

$$\mathcal{I}^{\star}_{dm,e_{i,j}}(P^{\star}_{i,j}, \mathcal{I}_{dm,a_{i,j}}) = \begin{pmatrix} \mathcal{I}^{\star}_{dm,e_{i,j}}\left(P^{\star}_{1,1}, \mathcal{I}_{dm,a_{1,1}}\right) & \mathcal{I}^{\star}_{dm,e_{i,j}}\left(P^{\star}_{1,2}, \mathcal{I}_{dm,a_{1,2}}\right) & \cdots & \mathcal{I}^{\star}_{dm,e_{i,j}}\left(P^{\star}_{1,J}, \mathcal{I}_{dm,a_{1,J}}\right) \\ \mathcal{I}^{\star}_{dm,e_{i,j}}\left(P^{\star}_{2,1}, \mathcal{I}_{dm,a_{2,1}}\right) & \mathcal{I}^{\star}_{dm,e_{i,j}}\left(P^{\star}_{2,2}, \mathcal{I}_{dm,a_{2,2}}\right) & \cdots & \mathcal{I}^{\star}_{dm,e_{i,j}}\left(P^{\star}_{2,J}, \mathcal{I}_{dm,a_{2,J}}\right) \\ \vdots & \vdots & \ddots & \vdots \\ \mathcal{I}^{\star}_{dm,e_{i,j}}\left(P^{\star}_{I,1}, \mathcal{I}_{dm,a_{I,1}}\right) & \mathcal{I}^{\star}_{dm,e_{i,j}}\left(P^{\star}_{I,1}, \mathcal{I}_{dm,a_{I,1}}\right) & \cdots & \mathcal{I}^{\star}_{dm,e_{i,j}}\left(P^{\star}_{I,J}, \mathcal{I}_{dm,a_{I,J}}\right) \end{pmatrix}. \quad (31)$$

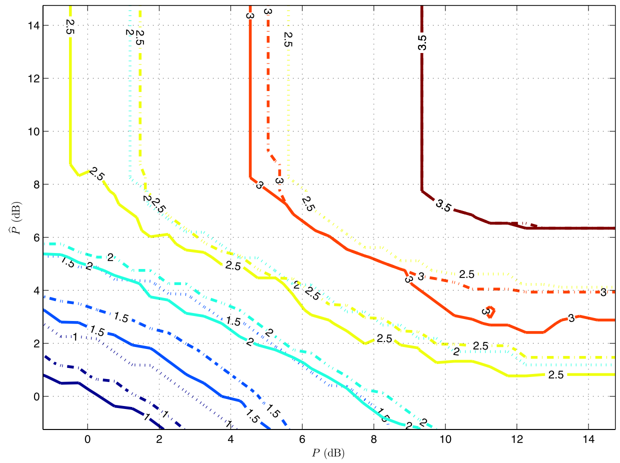

FIGURE 4. Hybrid channel throughput using AWGN optical(RF) channels. Regular structure (dotted lines), right-regular structure with partial optimization (dashed dotted lines), right-regular structure with full optimization (solid lines).

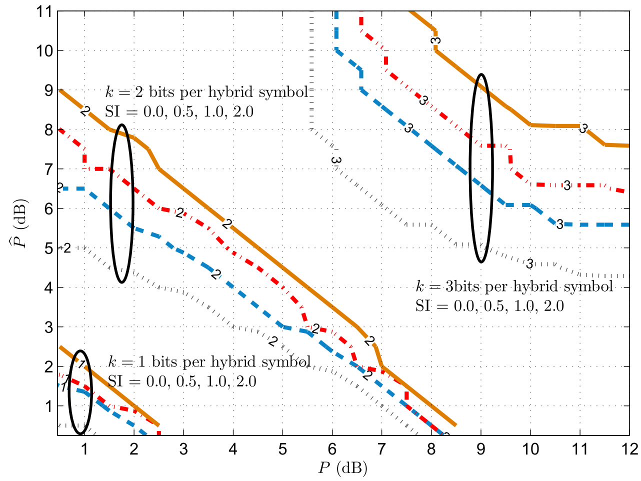

FIGURE 6. Hybrid channel throughput using AWGN RF and LN faded optical channels with varying SI considering partially optimized right-regular LDPC code. SI = 0 (dotted lines), SI = 0.5 (dashed lines), SI = 1.0 (dashed dotted lines) and SI = 2.0 (solid lines).

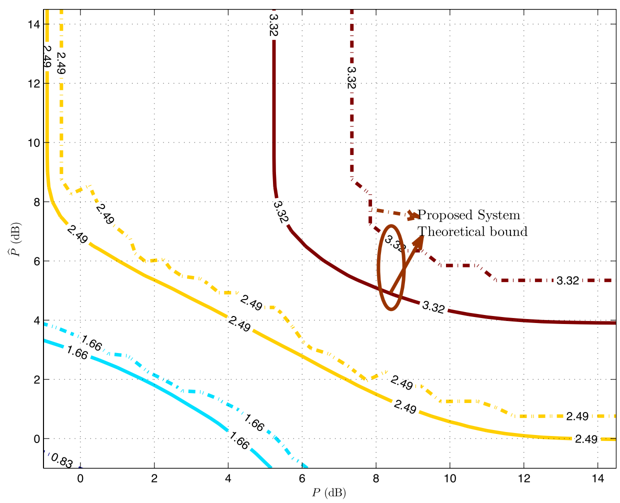

FIGURE 5. Comparison of TMA with fully optimized right-regular LDPC code (dash dotted lines) AWGN hybrid channel and theoretical bound (solid lines).

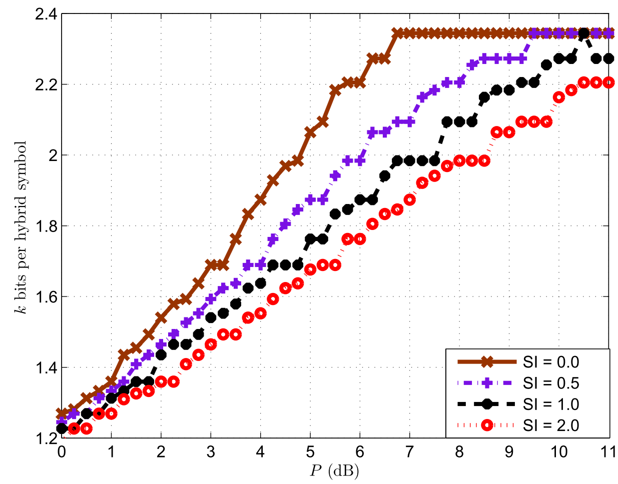

FIGURE 7. TMA with regular LDPC code considering fixed RF channel condition (i.e., $\widehat{P} = 5$ dB) and varying optical channel conditions.

using fully optimized right-regular structure, 1 dB more gain is possible as compared to right-regular structure with partial optimization and 2.25 dB compared to regular structure at $k = 1.5$ bits per hybrid symbol. It is also noted from Fig. 4 that two cases (i.e., full and partial optimization) are giving same performance at large power levels. The reason for that is, the algorithm selects quaternary modulations as the best modulation at large power level for each degree of VN.

In Fig. 5, it is seen that proposed TMA with fully optimized right-regular LDPC code is approaching the theoretical bound. The theoretical bound is generated using $\mathcal{I}_H = \mathcal{I}(P) + \widehat{\mathcal{I}}(\widehat{P})$, where $\mathcal{I}(P)$ and $\widehat{\mathcal{I}}(\widehat{P})$ calculated using [29] and [30, eq. (11)]. The gap from theoretical bound is about 1 dB at $k = 2.49$ bits per hybrid symbol and is about 2 dB at $k = 3.32$ bits per hybrid symbol.

Simulation results of throughput given by (28) are shown in Fig. 6 assuming right-regular LDPC code with partial optimization. AGM bit labelling for QPSK and 4-PAM in the respective AWGN RF channel and LN faded optical channel with SI $= \{0, 0.5, 1.0, 2\}$ is considered. In this way all other parameters of optical channel remains same except the SI is changed. By increasing SI, adaptive system selects small modulation size for different degree VN, while RF channel selects higher modulation sizes and in such situation more channel bits are sent through RF channel. The adaptive system even gives better performance improvement for using fully optimized right-regular LDPC code.

In Fig. 7, simulation results are given considering fixed RF channel condition (i.e., fixing RF channel power, while varying optical channel power) and also varying optical channel conditions by assigning different SI. It is seen that for large value of SI, throughput of system decreases significantly. Regular LDPC code and optimization function (13) is used to run simulation results shown in Fig. 7 and puncturing step size is 40. Such a large puncturing step size is used to get smooth results. It is seen that in order to achieve throughput of $k = 2$ bits per hybrid symbol, we need an optical power of 4.75 dB over SI = 0, while to get the same throughput over SI = 2, we need an optical power of 8 dB. Even more power gain is achieved by using right-regular LDPC code.

VI. CONCLUSION

Novel TMA is proposed for adaptive hybrid FSO-RF channel. Performance of proposed algorithm is analyzed for regular and right-regular LDPC code. AWGN RF channel is assumed while LN fading distribution along with AWGN signal model on optical channel is considered. It is seen that proposed algorithm well adopted to different weather scenarios and provides best throughput along with corresponding puncturing patterns. The adaptive system flexibly distributes amount of channel bits in an efficient way over varying optical channel conditions. It is noted that TMA performs well under all channel conditions and provides performance gain of up to 2.25 dB using right-regular LDPC code. The adaptive hybrid FSO-RF system selects its parameters (i.e., modulation selections, bit proportions for each channel and puncturing patterns for each degree VN) adaptively on varying optical channel conditions.

ACKNOWLEDGMENT

The author would like to thank Prof. Bill Cowley and Khoa D. Nyugen from ITR, UniSA, South Australia, for their suggestion and useful discussion during the whole journey of this research work.

REFERENCES

[1] M. A. Khalighi and M. Uysal, "Survey on free space optical communication: A communication theory perspective," *IEEE Commun. Surveys Tuts.*, vol. 16, no. 4, pp. 2231–2258, 4th Quart., 2014.

[2] M. Leba, S. Riurean, and A. Lonica, "LiFi—The path to a new way of communication," in *Proc. 12th Iberian Conf. Inf. Syst. Technol. (CISTI)*, Jun. 2017, pp. 1–6.

[3] H. T. T. Pham, N. T. Dang, L. T. Vu, and H. T. Bui, "A survey of performance improvement methods for free-space optical communication systems," in *Proc. Int. Conf. Adv. Technol. Commun. (ATC)*, Hanoi, Vietnam, Oct. 2014, pp. 770–775.

[4] I. S. Ansari, M. M. Abdallah, M. S. Alouini, and K. A. Qaraqe, "Outage performance analysis of underlay cognitive RF and FSO wireless channels," in *Proc. 3rd Int. Workshop Opt. Wireless Commun. (IWOW)*, Sep. 2014, pp. 6–10.

[5] Y. Zhang, B. Y. Kim, Y. Park, and K. D. Kim, "Performance analysis of hybrid FSO/RF system," in *Proc. Int. Conf. Ubiquitous Future Netw. (ICUFN)*, Jun. 2011, pp. 279–283.

[6] J. P. Soler, "Hybrid communication systems, FSO/RF and RoF: Reliable and scaled communications anywhere," in *Proc. Northumbria Res. Conf.*, Newcastle Upon Tyne, U.K., May 2011, pp. 1–3.

[7] D. Kedar and S. Arnon, "Urban optical wireless communication networks: The main challenges and possible solutions," *IEEE Commun. Mag.*, vol. 42, no. 5, pp. S2–S7, Feb. 2004.

[8] H. Izadpanah, T. Elbatt, V. Kukshya, F. Dolezal, and B. Ryu, "High-availability free space optical and RF hybrid wireless networks," *IEEE J. Sel. Areas Commun.*, vol. 10, no. 2, pp. 45–53, Apr. 2003.

[9] B. Makki, T. Svensson, T. Eriksson, and M.-S. Alouini, "On the performance of RF-FSO links with and without hybrid ARQ," *IEEE Trans. Wireless Commun.*, vol. 15, no. 7, pp. 4928–4943, Jul. 2016.

[10] Y. Tang, M. Brandt-Pearce, and S. G. Wilson, "Link adaptation for throughput optimization of parallel channels with application to hybrid FSO/RF systems," *IEEE Trans. Commun.*, vol. 60, no. 9, pp. 2723–2732, Sep. 2012.

[11] T. Rakia, H.-C. Yang, M.-S. Alouini, and F. Gebali, "Outage analysis of practical FSO/RF hybrid system with adaptive combining," *IEEE Commun. Lett.*, vol. 19, no. 8, pp. 1366–1369, Aug. 2015.

[12] M. M. Abadi, Z. Ghassemlooy, S. Zvanovec, M. R. Bhatnagar, and Y. Wu, "Hard switching in hybrid FSO/RF link: Investigating data rate and link availability," in *Proc. IEEE Int. Conf. Commun. Workshops (ICC Workshops)*, May 2017, pp. 463–468.

[13] H. Al-Quwaiee, I. S. Ansari, and M.-S. Alouini, "On the performance of free-space optical communication systems over double generalized gamma channel," *IEEE J. Sel. Areas Commun.*, vol. 33, no. 5, pp. 1829–1840, May 2015, doi: 10.1109/JPHOT.2017.2723422.

[14] I. S. Ansari, M. S. Alouini, and J. Cheng, "On the capacity of FSO links under lognormal and Rician-Lognormal turbulences," in *Proc. IEEE 80th Veh. Technol. Conf. (VTC-Fall)*, Vancouver, BC, Canada, Sep. 2014, pp. 1–6, doi: 10.1109/VTCFall.2014.6966082.

[15] H. Lei, Z. Dai, I. S. Ansari, K. H. Park, G. Pan, and M. S. Alouini, "On secrecy performance of mixed RF-FSO systems," *IEEE Photon. J.*, vol. 9, no. 4, pp. 1–14, Aug. 2017, doi: 10.1109/JPHOT.2017.2723422.

[16] I. S. Ansari, M. M. Abdallah, M. S. Alouini, and K. A. Qaraqe, "A performance study of two hop transmission in mixed underlay RF and FSO fading channels," in *Proc. IEEE Wireless Commun. Netw. Conf. (WCNC)*, Istanbul, Turkey, Apr. 2014, pp. 388–393, doi: 10.1109/WCNC.2014.6952039.

[17] M. N. Khan, M. Jamil, and M. Hussain, "Adaptation of hybrid FSO/RF communication system using puncturing technique," *Radioengineering*, vol. 25, no. 4, pp. 12–19, 2016.

[18] M. N. Khan and M. Jamil, "Adaptive hybrid free space optical/radio frequency communication system," *Telecommun. Syst.*, vol. 65, no. 1, pp. 117–126, Aug. 2017.

[19] M. N. Khan and M. Jamil, "EXIT chart behaviour for the hybrid FSO/RF communication system," in *Proc. 10th Int. Conf. Inf., Commun. Signal Process. (ICICS)*, Dec. 2015, pp. 1–5.

[20] M. A. Amirabadi and V. T. Vakili. (Mar. 2018). "Performance of a relay-assisted hybrid FSO/RF communication system." [Online]. Available: https://arxiv.org/abs/1803.00711

[21] M. A. Amirabadi and V. T. Vakili. (Feb. 2018). "A novel hybrid FSO/RF communication system with receive diversity." [Online]. Available: https://arxiv.org/abs/1802.07348

[22] L. C. Andrews and R. L. Phillips, *Laser Beam Propagation Through Random Media*. Bellingham, WA, USA: SPIE Press, 2005.

[23] M. V. Jamali *et al.*, "Statistical distribution of intensity fluctuations for underwater wireless optical channels in the presence of air bubbles," in *Proc. Iran Wssorkshop Commun. Inf. Theory (IWCIT)*, May 2016, pp. 1–6.

[24] S. Ten-Brink, "Designing iterative decoding schemes with the extrinsic information transfer chart," *AEU Int. J. Electron. Commun.*, vol. 54, no. 6, pp. 389–398, 2000.

[25] F. R. Kschischang, B. J. Frey, and H.-A. Loeliger, "Factor graphs and the sum-product algorithm," *IEEE Trans. Inf. Theory*, vol. 47, no. 2, pp. 498–519, Feb. 2001.

[26] O. Alamri, J. Wang, S. Ng, L.-L. Yang, and L. Hanzo, "Near-capacity transceiver design using exit-curve fitting: Three-stage turbo detection of irregular convolutional coded joint sphere-packing modulation and space-time coding," in *Proc. IEEE ICC*, Jun. 2007, pp. 4028–4033.

[27] S. ten Brink, G. Kramer, and A. Ashikhmin, "Design of low-density parity-check codes for modulation and detection," *IEEE Trans. Commun.*, vol. 52, no. 4, pp. 670–678, Apr. 2004.

[28] H. Chen, R. G. Maunder, and L. Hanzo, "Lookup-table-based deferred-iteration aided low-complexity turbo hybrid ARQ," *IEEE Trans. Veh. Technol.*, vol. 60, no. 7, pp. 3045–3053, Sep. 2011.

[29] R. G. Gallager, *Information Theory and Reliable Communication*, 2nd ed. New York, NY, USA: McGraw-Hill, 1968.

[30] M. N. Khan, A. Rafay, S. O. Gilani, and M. Jamil, "Link adaptation for maximizing MI of hybrid optical/RF communication system," *Procedia Comput. Sci.*, vol. 110, pp. 282–289, Jul. 2017.

MUHAMMAD NASIR KHAN received the B.E. degree in electronic engineering from the Dawood University of Engineering and Technology, Karachi, Pakistan, in 2002, the M.Sc. degrees (Hons.) in communication engineering from the University of Engineering and Technology Lahore, Pakistan, and the Technical University of Delft, The Netherlands, in 2007 and 2009, respectively, and the Ph.D. degree in telecommunications from the Institute for Telecommunication Research, University of South Australia, Australia, in 2013. He is currently a Professor with the Electrical Engineering Department, The University of Lahore, Pakistan. His research interests include channel coding, detection theory, development of energy efficient algorithm for wireless sensor network, signal processing for communication, advance metering infrastructure, and optimization techniques.

SYED OMER GILANI received the M.Sc. degree in computer engineering from Dalarna University, Sweden, in 2006, and the Ph.D. degree in electrical and computer engineering from the National University of Singapore in 2013. From 2006 to 2008, he was with the Interactive Multimedia Laboratory, Singapore. He is currently an Assistant Professor with the National University of Sciences and Technology, Pakistan. His research interests include human–machine interaction and networking. He actively consults for industries on various projects.

MOHSIN JAMIL received the B.Eng. degree in industrial electronics from NED University, Pakistan, in 2004, the master's degrees from Dalarna University, Sweden, and the National University of Singapore in 2006 and 2008, respectively, and the Ph.D. degree from the University of Southampton, U.K., in 2011. He was an Assistant Professor with the Department of Robotics and AI, National University of Sciences and Technology, Islamabad, Pakistan. He is currently an Associate Professor with the Department of Electrical Engineering, Islamic University of Medina, Saudi Arabia. His research interests include control design, myoelectric control, soft switching techniques, and smart grid technologies.

ABDUL RAFAY received the B.Sc. and M.Sc. degrees in electrical engineering from The University of Lahore, Lahore, Pakistan, in 2012 and 2017, respectively. He is currently a Lecturer with the Electrical Engineering Department, The University of Lahore. He is an External Researcher with the National University of Sciences and Technology, Islamabad, Pakistan. His research interests include detection schemes, communication theory, and wireless communication and networking.

QASIM AWAIS received the B.Sc. degree in electronics engineering from the University of Engineering and Technology, Taxila, Pakistan, in 2009, and the M.Sc. degree in computer networking from the University of Bedfordshire, U.K., in 2011. He is currently pursuing the Ph.D. degree in instrumentation science and technology with Chongqing University, China. His research interest includes wide band/multiband antenna design, renewable energy systems, RF energy harvesting, RF filter design, and multisource energy scavenging/integration.

BILAL A. KHAWAJA received the B.S. degree in computer engineering from the Sir Syed University of Engineering and Technology, Karachi, Pakistan, in 2002, the M.Sc. degree in communication engineering and signal processing from the University of Plymouth, Plymouth, U.K., in 2005, and the Ph.D. degree in electrical engineering from the University of Bristol, Bristol, U.K., in 2010. His research interests are in the next generation of millimeter-wave (mm-wave) radio-over-fiber and optical communication systems, mm-wave and THz signal generation mode-locked lasers and RF transceiver design and antennas design/characterization for Wi-Fi/IoT/UAVs/FANETs/5G systems/UWB wireless body area networks, wireless sensor networks, and mm-wave frequency bands.

MUHAMMAD UZAIR received the B.Sc. degree in electrical engineering from the University of Engineering and Technology, Lahore, Pakistan, in 1996, the M.Sc. degree in electrical engineering from Concordia University, Montreal, QC, Canada, in 2005, and the Ph.D. degree in electrical engineering from the University of Guelph, Guelph, ON, Canada, in 2014. He is currently an Assistant Professor with the Faculty of Engineering, Islamic University of Madinah, Medina, Saudi Arabia. His research interests include image/video and signal processing, developing algorithms for solving engineering problems and medical applications, developing wireless protocols, and wireless video optimization.

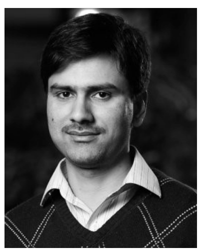

ABDUL WAHEED MALIK received the M.Sc. degree in electrical engineering from Linkoping University in 2009 and the Ph.D. degree in electronics design from Mid Sweden University, Sweden, in 2014. He is currently an Assistant Professor with the Islamic University of Madinah, where he is teaching in the area of digital design and embedded systems. He is a Faculty Member of COMSATS University Islamabad. He has published in the areas of machine vision and image processing from the last seven years. His research interests are hardware architecture design for real-time image processing systems, machine vision, and machine learning algorithms.